Journal of Mechanics Engineering and Automation 4 (2014) 412-421

A Wind Tunnel Two-Dimensional Parametric Investigation of Biplane Configurations

Miguel Ángel Barcala-Montejano, Ángel Antonio Rodríguez-Sevillano, María Elena Rodríguez-Rojo and Sara Morales-Serrano

Department of Aerotecnia, Technical University of Madrid, Madrid 28040, Spain

Received: January 09, 2014 / Accepted: February 07, 2014 / Published: May 25, 2014.

Abstract: This paper presents an experimental and systematic investigation about how geometric parameters on a biplane configuration have an influence on aerodynamic parameters. This experimental investigation has been developed in a two-dimensional approach. Theoretical studies about biplanes configurations have been developed in the past, but there is not enough information about experimental wind tunnel data at low Reynolds number. This two-dimensional study is a first step to further tridimensional investigations about the box wing configuration. The main objective of the study is to find the relationships between the geometrical parameters which present the best aerodynamic behavior: the highest lift, the lowest drag and the lowest slope of the pitching moment. A tridimensional wing-box model will be designed following the pattern of the two dimensional study conclusions. It will respond to the geometrical relationships that have been considered to show the better aerodynamic behavior. This box-wing model will be studied in the aim of comparing the advantages and disadvantages between this biplane configuration and the plane configuration, looking for implementing the box-wing in the UAV's field. Although the box wing configuration has been used in a small number of existing UAV, prestigious researchers have found it as a field of high aerodynamic and structural potential.

Key words: Biplane, two-dimensional, box-wing, aerodynamic behavior, wind tunnel test.

Nomenclature

C_L	Lift coefficient
C_D	Drag coefficient
C_{Di}	Induced drag coefficient
α	Angle of attack
C_L/C_D	Lift-to-drag ratio
C_m	Pitch moment coefficient
AR	Wing aspect ratio
e	Wing span efficiency factor
V_∞	Wind tunnel test section freestream velocity
V_c	Corrected velocity in the wind tunnel test section due to blockage effects
ε	Correction factor for blockage effects
A_{wing}	Wing area
A_{TS}	Test section area
δ_w	Boundary correction factor
p	Air density
A	Box-wing wing area
A	$2A_{wing}$
c	Wing chord
L	Lift force
D	Drag force
M	Pitching moment

Corresponding author: Ángel Antonio Rodríguez-Sevillano, Ph.D., research fields: wind tunnel testing, preliminary and conceptual design in the field of rpas, and flow visualization. E-mail: angel.rodriguez.sevillano@upm.es.

1. Introduction

In the last years, new aircraft configurations [1-4] have been studied aiming to achieve improvements in the aircraft performance. "The presently dominant configuration can no longer be improved, making the end of progress'', Torenbeek [5, 6] said.

The main way of improving the aerodynamic behaviour of an aircraft is to decrease its drag force. The latest studies in this field focus on configurations with lower induced drag than the present ones.

Nonplanar wings achieve a reduction of induced drag compared with planar wings of the same span and lift [3]. There are numerous nonplanar

configurations to consider as candidates to be studied as a way of reducing drag. Although, the one which achieves the minimum induced drag for a given lift, span and vertical extent, is the box-wing configuration. This fact is represented by the value of the span efficiency factor *e*, as shown in Fig. 1.

$$C_{Di} = \frac{C_L^{\,2}}{\pi ARe} \tag{1}$$

Induced drag is the drag due to lift. The drag associated with lift accounts for roughly half of the total drag when the airplane is flown at the condition leading to maximum lift-to-drag ratio. In the take-off and landing conditions, this drag is predominant, but at cruise condition, the speed is higher than the one corresponding to the maximum efficiency, so the parasite drag governs the total drag.

Our work deals with UAS (unmanned aerial systems) [7] in the low Reynolds number regime [8]. This implies low velocities and low sizes, because the airplanes that we work with do not have span longer than one meter. These two characteristics imply that the parasite drag becomes more relevant. Introducing a biplane configuration as the box-wing, will increase the wetted surface, so the parasite drag will increase also, while the induced drag decreases. We will have this fact into account in the three dimensional future study; our objective is to determine if the reduction of induced drag obtained with the box-wing configuration is bigger or smaller than the increase of the parasite drag. Thus, we will consider if we obtain a reduction or an increase of the total drag with the introduction of the box-wing configuration for low Reynolds numbers.

The reduction of the induced drag is not only the possible advantage to obtain in the box-wing configuration; in addition, a bigger lift could be obtained for a box-wing with the same span than a planar wing. Also, the need in the UAS world of portability arises. In the UAS field, the increase of lift and the reduction of induce drag cannot be obtained with a simple increase of span; the airplanes must be easy to transport by a person by foot (in the field of UAS, the conceptual design of MOLLE (modular lightweight load-carrying equipment)).

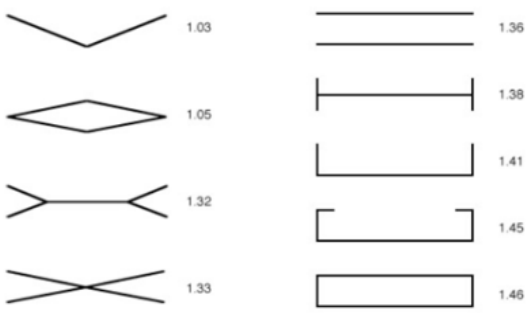

Fig. 1 Wing Span efficiencies for various optimally loaded nonplanar systems (*h*/*b* = 0.2) [1].

Different combinations of geometrical parameters in biplane configurations lead to different aerodynamic behaviour. A systematic study of these parameters has carried out.

A two dimensional model was designed, in which four geometric parameters can be modified: the gap, the stagger, the angle of incidence and the sweep. The gap is the vertical distance between the quarter chord points of each wing. The stagger is the longitudinal distance between the quarter chord points of each wing, positive if the upper wing is forward the lower wing. The incidence is the angle of each wing between a reference position and the flow direction. And the sweep is the angle between the quarter chord line of the wing and the perpendicular line to the plane symmetry of the airplane.

The model has been tested in a three-dimensional wind tunnel. As the study is a two-dimensional one, two end plates have been added at both sides of the model, trying to achieve a two dimensional flow conditions. Geometrical parameters have changed systematically during the tests. The total aerodynamic forces and pitching moment have been measured in all the cases.

It has to be taken into account that in a bi-dimensional model the induced drag cannot be considered. The model tested is a first step in the study of the box-wing configuration. The main

advantage of the box wing configuration against the planar configuration, the reduction of induced drag, would have to be study in a three dimensional model.

Therefore, in this document we only present the work related to the two dimensional study of a biplane configuration, in which the planes can take different relative positions.

The experimental work's objective is to conclude which relationship between parameters is the one that maximizes the lift, and minimizes the drag and the slope of the pitching moment.

Once this relationship was chosen, a three dimensional model has been designed. With this model, we will determine the reduction of drag between the box wing and the planar configuration, the height to span ratio variation, the stability of the vehicle and the structural characteristics.

One of the most important objectives related to the structural characteristics, is to work out if they can reduce the total drag. If it obtained, it could lead to an increase of the range or endurance of the airplane, bigger than the reduction that in these aerodynamic variables would cause the possible increase of weight of the biplane configuration against the planar configuration. According to Ref. [9], a 24% lighter aircraft could be designed using a nonplanar configuration. The Miranda's box-wing configuration [10] covers a minimum induced drag along with structural and stability benefits.

We will use the theoretical studies to help us in the final choose of all the geometrical parameters of the three dimensional model of the box wing.

The theoretical studies about box-wing can be resuming in three formulations:

- The minimum induced drag configuration has the same span loading on each wing, and a lift distribution which approaches zero at the midpoint of the vertical planes; the lift distribution in the wings is the addition of a constant lift distribution and an elliptical distribution [11-13]. This wing configuration is called the Prandtl's best wing system;
- If the lift distribution or circulation is held constant, the total induced drag of the system is unaffected by changes in the longitudinal position of the elements. This theorem was enounced by Munk [14] in 1921, and it is known as Munk's Stagger Theorem. The theorem implies that box-wing design is independent of sweep and stagger if the correct span loading is maintained;
- The induced drag decreases for increasing non-dimensional gaps [15];
- Height to span ratio variation is the most important design variable for a box-wing aircraft [16]. If a single wing is separated into two wings, with the same total area and span than this wing, maximum induced drag reduction is achieved [17]. That is because aspect ratio has been doubled, and an increase in aspect ratio reduces the induced drag. This reduction goes bigger as the gap increases, because the interference factor between the two wings decreases.

With changes in the stagger and sweep, lift distribution changes, as it does with changes in gap, angle of incidence and twist. The stagger, the gap and the sweep, are fixed geometrical parameters in the three dimensional model. Helped by vortex lattice programs, we will determine the angle of incidence of each wing and the twist which lead to the most similar load distribution to that mentioned in the Prandtl's best wing system. The Munk's Stagger Theorem assure us that we could find the load distribution that leads to minimum induced drag, because in our model the only parameters that have been changed against the Prandtl's configuration are longitudinal parameters, the stagger and the sweep.

Using this model, we would like to determine the advantages and disadvantages between the planar configuration, used nowadays in airplanes as a way of reducing drag, and the box-wing configuration. The model includes planar and box-wing configurations. The planar configuration is a wing with winglet devices at the tips. It is the upper forward wing of the

box-wing configuration. The aft lower wing is attached to the first wing and the fuselage, to achieve the box wing configuration. The model has also a removal tail, for being used, if necessary. The wings in the box-wing system have nearly the same span and total area as the monoplane's wing; the lower wing only differs from the upper wing in the winglet segment.

The characteristics of the upper wing and the wing of the monoplane configuration have obtained in Ref. [18], which deals with how to obtain the optimal nonplanar lifting surfaces. These authors vary a number of wing elements, and use a panel method and a beam finite-element model, helped both by an augmented Lagrangian particle swarm optimizer, aiming to solve the multidisciplinary aero-structural optimization problems. They found that, only when aerodynamics are considered, closed lifting surfaces, as box-wing and joined-wing, are the optimal ones, which minimize the drag. However, when aero-structural optimization is performed, a winglet configuration is found to be optimal, with an overall span constrained, and a wing with a raked wingtip is optimal, with no constrained span.

We have chosen the winglet wing as the planar configuration, because the span is constrained by the dimensions of the wind tunnel where the model is tested. The wing's dimensions have been calculated based on the dimensions of the mentioned paper.

The box-wing geometrical parameters have been chosen in accordance to the conclusion of the experimental study, selecting the confluence of parameters, which minimize the drag and the total moment in the arm of the model, and have the highest lift.

As our work focuses on UAS systems, the fuselage and the tail have been designed using other UAS as reference, such as the Outrider or the D1.

In conclusion, with the experimental study, shown bellow in this document, we have chosen the relationship between four geometrical parameters which has an optimum response in the maximization of the lift, along with the minimization of the drag and the slope of the pitching moment. With the two main parameters frozen (the gap and the stagger, along with the sweep), we have designed a three dimensional model of a box wing, joined to a planar configuration, so we can compare both in the same model. We hope the box-wing configuration to provide a higher lift than the planar wing, in addition with a reduction of induced drag. Besides, it will introduce a bigger wetted surface than the planar configuration, so the parasite drag will increase for the box-wing configuration. As we work in the range of low Reynolds numbers, the parasite drag has an important role in the total drag of the airplane. With the three dimensional models, we will consider if the reduction of the induced drag due to the box wing configuration is capable of reducing the total drag, or the increase of the parasite drag is bigger. Furthermore, we will study if the increase in lift and the decrease in drag mentioned, have a bigger influence in the performance of the airplane than the increase in structural weight. Also, it will be considered if lose of weight related to the disappearance of the tail, horizontal and vertical stabilizers, could balance the addition of a second wing and lateral planes in the box-wing configuration, against the planar configuration. Finally, the stability will be considered.

The paper is organized as follows: First, we introduce the experimental apparatus used in the study, the wind tunnel and the bi-dimensional model; Secondly, we describe the experimental procedure, talking about wind tunnel corrections applied and the tested model characteristics; Thirdly, we show the results, related with how the geometrical changes affect the aerodynamic behavior of the model; Finally, we introduce the conclusions, which summarize the optimum geometrical relationships, presenting the basis of the future box-wing design.

2. Experimental Apparatus

The model consists of four wings, two with sweep angle and two without sweep. All of them have been manufactured by a CAD/CAM milling machine, of Necuron material. The airfoil selected has been the Eppler387, appropriate for low Reynolds numbers. The chord of the wings is a constant one, with a value of 0.175 m. The span of the wings is 0.140 m, parameter which is not relevant because we have worked with a two-dimensional flow.

The wings have at both sides a pair of aluminium narrow plates, which allow changing the incidence during the tests and strengthening the union between the wings and the lateral model plates. The model is showed in Fig. 2. The wings have two holes, one aligned with the quarter chord point of the root chord, and the other one at a distance of a chord from the first one. This second hole permits the change of angle of incidence, rotating the wing around the first hole. Screws have been used to fix the positions. In the lateral plates of the model, three holes have been situated in a straight line. The variation of the incidence of the wing has been achieved by changing the matching between the second hole of the plates in the wing and one of the three holes in the end-plates of the model. The biggest difference of incidence between the upper and lower wing is ±6 degrees (shown in Fig. 5).

The lateral aluminium plates of the model have a 1.5 mm width. They assure a two dimensional flow condition during the tests and support the wings, allowing the changes of the geometrical parameters. They present three vertical positions, permitting the variation of the gap in a one and a half chord distance. They also present longitudinal holes which allow the change of longitudinal parameters (Fig. 3 and 4), such as sweep and stagger. Finally, in some longitudinal positions, additional holes have been made to permit an interval of incidence angle variations.

The union of the model to the wind tunnel balance is by means of a sting end which parts from one of the lateral plates (a sting ended connection mounted on one of the lateral plates links the model with the wind tunnel balance). The plate which allows the attachment with the balance represents the fuselage-wing union. The wings with sweep have been

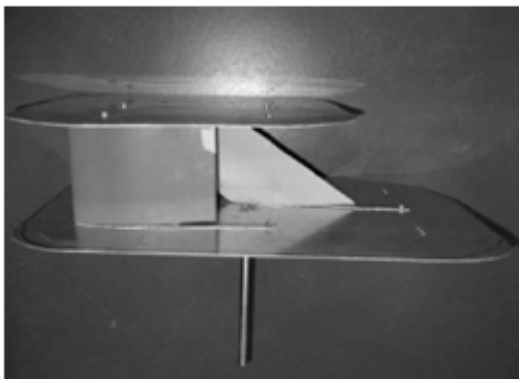

Fig. 2 Upper view of the entire test model.

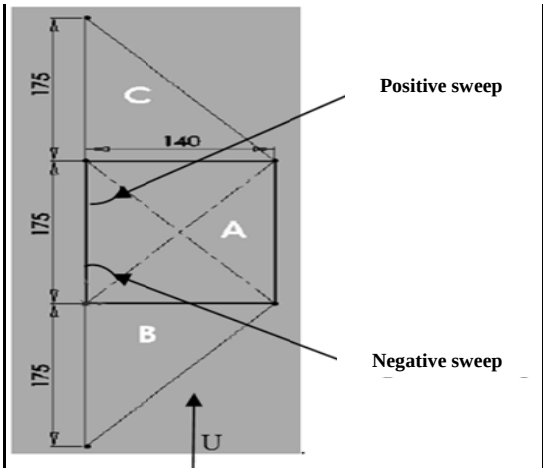

Fig. 3 Plant view of the different sweep configurations.

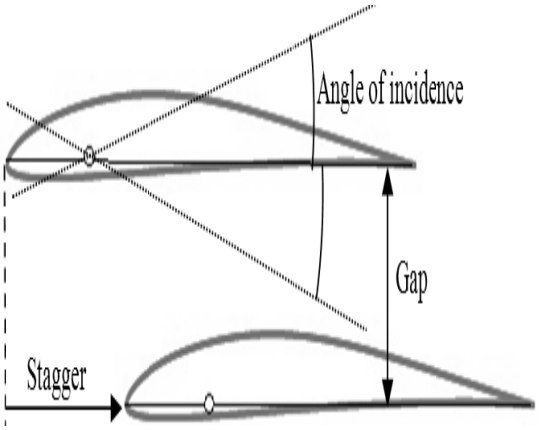

Fig. 4 Geometrical parameters.

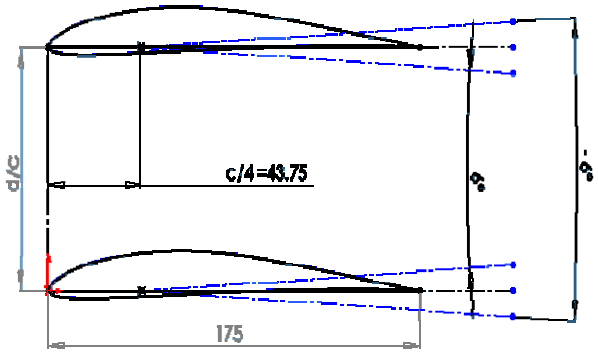

Fig. 5 Relative angle of incidence between the wings.

moved forward or backwards in this plate to achieve the desired configuration. On the other plate, there is no difference in the longitudinal position of the leading edge of the wings.

The wind tunnel involved in the tests is a low speed open return wind tunnel; it is open on both ends and draws air from the laboratory into the closed test chamber (square section), used for three dimensional tests. It discharges directly to the laboratory, thus the pressure in the tunnel is nearly the atmospheric pressure in the laboratory, preventing blockage problems. The range of the tunnel airspeed is between 0 m/s and 33 m/s. The models have been mounted on one of the tunnel walls, with the balance placed on this lateral position, which allows one degree of freedom; it permits the change of the pitch angle. This balance gives three forces measurements, two lift components (with these two components we can calculate pitching moment value), and one drag component.

The wind tunnel is provided with an electronic transducer. This device allows measuring the wind tunnel speed, through the differential pressure gauge between static and total pressure (using Bernoulli equation).

The aerodynamic forces acting on the model are transmitted to the wind tunnel balance, and from there they are recorded by the data hardware. This hardware converts analogical signals, corresponding to the measurements of the forces, to digital signals. These digital signals are again transmitted to the data software, Labview3.3.c, which presents and stores the results on a computer.

3. Experimental Procedure

3.1 Wind Tunnel Corrections

There are two main corrections to be done in the wind tunnel measurements.

First, the blockage effects have to be considered. They are estimated with the ratio of frontal area of the model to the wind tunnel test section cross-sectional area. The ratio resulted has to be lower than the maximum admissible ratio [19]. The wind tunnel test section freestream velocity V_∞, is corrected for the blockage effects to give V_C.

$$V_c = (1+\varepsilon)V_\infty \tag{2}$$

where, ε is the correction factor for blockage effects:

$$\varepsilon = 0.25 \times \frac{\text{model frontal area}}{\text{test section area}} \tag{3}$$

Secondly, the corrections for the wall interference have to be studied. Wind tunnel walls induced interference can partly be eliminated by applying angle-of-attack corrections. One of the most frequently used corrections is the Glauert correction methodology [20]. It is considered to be the classical correction method for wind tunnel tests with fixed wing models. In addition, the angle-of-attack corrections can be found by utilizing other flow theories, like the Heyson and Brooks correction methodologies [21, 22], or by experimental procedures data.

In the Glauert correction methodology, the induced angle correction is in the form:

$$\Delta\alpha = \left[\frac{\delta_w A_{wing}}{A_{TS}}\right] C_L \tag{4}$$

The wing area is represented by A_{wing}, A_{TS} is the test section area, C_L is the lift coefficient and δ_w is the boundary correction factor.

The boundary factor δ_w, is dependent on the test section shape, the ratio of the wing span to tunnel width, and the position of the wing in the test section.

In the present work, no correction has been applied. The purpose of the study is to compare the results of

each configuration, not to obtain the exact results of each campaign. If in further studies there is the need of higher accuracy, the corrections will be introduced.

3.2 Tested Model Characteristics

There are five configurations, each of them differing to the rest in the stagger and the sign of the sweep. The stagger takes three values: zero and once the chord length, with negative and positive sign. The positive sign of the stagger corresponds to the cases where the leading edge of the upper wing root chord is forward the leading edge of the root chord of the lower wing. The value of the sweep is 50°, with positive or negative sign.

In these configurations, during the test runs, the gap and the angle of incidence are varied. The five configurations have been distinguished with a pair of capital letters. The letter "A" represents no sweep, letter "B" represents negative sweep and letter "C" represents positive sweep (Fig. 3). The order of the two letters is also important: the first position indicates that the wing is the upper one, and the second place represents that the wing is the lower one. In the configurations there are always a wing swept and a no swept wing, except for the run with the two wings without sweep. The leading edge of the root chord of the wings with sweep is one chord distance backward or forwards the leading edge of the root chord of the wing without sweep.

Examples of these configurations are: AA, $St = 0$; AB, $St > 0$; AC, $St > 0$; BA, $St < 0$; CA, $St > 0$.

The variation of the gap has been represented by two values: one chord length and half a chord length. In the nomenclature of the wing configuration, the specification of the gap goes after the two capital letters: "10" represents a gap of a chord distance, and "05" represents a gap of a half chord distance.

With one of the five configurations selected and a gap distance fixed, the difference between the angles of incidence of both wings has been varied. It is specified by adding at the end of the model denomination the value of the relative incidence: ±6, ±3, 0.

Here is a pair of example of the nomenclature:

- AB05 + 6

A—Upper wing without sweep

B—Lower wing with negative sweep, forward the upper wing, therefore, the stagger is negative

05—Gap with a half chord distance value

+6—Relative angle of incidence of +6□

- AA100

A—Upper wing without sweep

B—Lower wing without sweep

10—Gap with once chord distance value

0—Relative angle of incidence of 0□

Finally, with one of the five configurations chosen, one gap distance and a relative incidence fixed, the last parameter that has been changed is the angle of attack of the model. This variation has been made by rotating a graduated wheel of the balance; the sting part of the model attached to the balance rotates with this wheel, producing the rotation of the entire model. The angle of attack varies from -15□ to +24□. This angle has been referred to the upper wing (the lower one in the position into the test section) position at the beginning of the run; if this wing has 3□ of incidence in the run, the angle of attack varies between -18□ and +21□.

Following this test procedure, fifty runs have been made.

Before any test was made, the calibration of the balance was completed. Tests have been run without freestream velocity to establish the initial conditions of the experiment.

The airspeed velocity for all the runs has been fixed between 20 m/s and 25 m/s, aiming to achieve a Reynolds number of 210,000.

The results obtained have been lift, drag and pitch moment. With these forces, the lift, drag and moment coefficients have been calculated.

$$C_L = \frac{L}{\frac{1}{2}\rho V_\infty^2 A}, \quad C_D = \frac{D}{\frac{1}{2}\rho V_\infty^2 A}, \quad C_M = \frac{M}{\frac{1}{2}\rho V_\infty^2 Ac} \quad (1)$$

The moments have been measured related to the union shaft between the balance and the model. The point of force application will be the quarter chord point of the upper wing of the configuration, the lower one in the test position. The variable A corresponds to twice the wing surface of one wing of the model.

4. Results

The variables that have been intended to be studied are: $C_{L\max}$, $C_{D\min}$, $(C_L/C_D)_{\max}$, $\mathrm{d}C_M/\mathrm{d}\alpha$, $\mathrm{d}C_L/\mathrm{d}\alpha$.

The lift coefficient $C_{L\max}$, represents the ability of a wing configuration for giving lift. The more lift it provides, the more weight the aircraft can support, and the lower is the stall velocity.

Low values of the drag coefficient $C_{D\min}$, imply less energy that the wing configuration looses in its interaction with the flow. Lower loss of energy allows bigger endurance and range of the aircraft provided with this wing configuration.

High values of the aerodynamic efficiency, $(C_L/C_D)_{\max}$, lead to more efficient flights. In a jet airplane, the maximum value of this ratio corresponds to a maximum endurance; in a propeller aircraft, the maximum corresponds to a maximum range.

Three relationships between the variable parameters have been established, in order to easily understand the behavior of the model. The three scenarios have been examined plotting up the curves of the following pair of variables:

$$C_L - \alpha;\ C_D - C_L;\ C_L/C_D - C_L;\ C_M - \alpha$$

For each scenario, the following conclusions have been obtained:

- Relative incidence and stagger have been maintained constant; the gap changes. The bigger the gap is, the better the results obtained for all the variables implied;
- Relative incidence and gap have been maintained constant; the stagger changes. The better behavior has been observed for positive staggered configurations, with the lower wing with positive sweep (configuration AC). The non staggered configuration AA, has achieved the best results in the aerodynamic efficiency coefficient. The configuration with minimum slope of the moment coefficient has been the AC configuration;
- The stagger and gap have been maintained constant; the relative incidence changes. The change of the incidence angle has not affected strongly the performance of the wing configuration;
- The stagger has been maintained constant; the relative incidence and gap change. In almost all cases, the configuration which has shown the best behavior has been the configuration of one chord length; it has been the biggest value of the gap tested in the whole series of experiments. The influence of the angle of incidence in the behavior of the configurations should not clearly state a criterion;
- The relative incidence has been maintained constant; the stagger and gap change. The configurations with better performances have been AA10 and AC10. Only in the analysis of the moment coefficient slope, the half chord gap has achieved better results than the one chord gap. That is because the moments in the quarter chord point of the upper wing will be lower if the wings are closer;
- The gap has been maintained constant; the relative incidence and stagger change. The configurations AA and AC have been the ones with better performance results. With respect to the incidence angle, there has not been a clear enough pattern to establish;
- The maximum lift coefficient slope has been examined. The configuration with the highest slope has been the AA10-3 configuration.

5. Conclusions

In this section, we present the main conclusions related to:

$C_{L\max}$, $C_{D\min}$, $(C_L/C_D)_{\max}$, $\mathrm{d}C_M/\mathrm{d}\alpha$, $\mathrm{d}C_L/\mathrm{d}\alpha$.

The maximum values of the lift coefficient, versus the angle of attack, have been obtained for the configurations AC10 + 3, AC050, AC100 and AC05 + 3.

The minimum values for the drag coefficient have been observed in the configurations AA10 − 3 and AC10 + 3.

The maximum values of aerodynamic efficiency have been obtained for the configurations AA100 and AA10 − 3.

The pitching moment coefficient has been referred to the quarter chord point of the upper wing root, instead of being referred to the aerodynamic centre. Even though conclusions for the coefficient curve slope have been obtained, the lower the curve slope is, the better behavior the configuration will have to longitudinal perturbations. The configurations with the lowest slopes in the graphs of moment coefficient versus angle of attack have been AC05 + 6 and AC05 + 3.

Finally, the configuration with a highest lift coefficient slope has been the AA10 − 3 configuration.

The predominant gap value is the one chord value, though the half chord gap obtains better results in the moment coefficient slope.

With regards to the relative incidence, clear conclusions cannot be obtained yet.

Taking into account the points reflected above, the configuration AC shows good results for maximum lift coefficient and minimum drag coefficient, in addition to the best response in the minimization of the pitching moment coefficient slope.

With the aim of designing a three dimensional model, the AC10 configuration has been chosen. The advantages of this configuration versus the configuration without stagger (AA) are related to the stability and the higher maximum lift coefficient. It also presents a minimum drag coefficient, as the AA biplane configuration. Another advantage, not related with the previous variables, is the higher pitching control capability of this wing configuration. A configuration like the AC could have control during flight without additional control surfaces, as the horizontal and vertical stabilizers. The aft wing could act as the elevator. In the lateral planes, union between both wings, there could be mobile surfaces which act as rudders. The inclusion of the controls in the wing would save a lot of weight.

As it has already been mentioned, the three dimensional model includes two configurations, the planar configuration with the upper wing and tail, and the box-wing configuration, with upper and lower wing and without tail. The design of the three dimensional model is based on box-wing of UAS in service, such as the outrider and the D1. The upper forward wing design can be found in Ref. [16].

With this model, the authors [23-25] intent to undertake a further study of the box-wing configuration, comparing it with the nowadays wing configuration. We will try to establish the advantages and disadvantages between the aerodynamic response of the wing with winglets and the box-wing. We will also hope to obtain the structural and stability analysis of both configurations, to study the differences in this field.

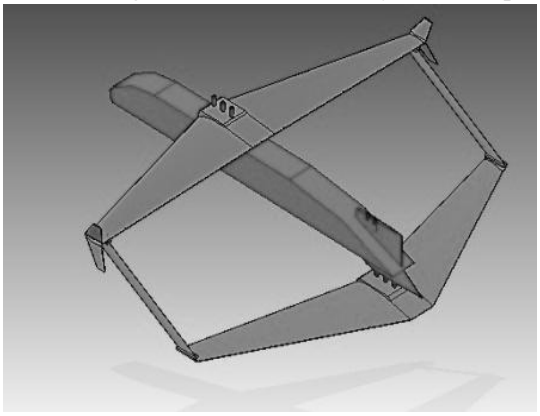

Fig. 6 Box-wing configuration.

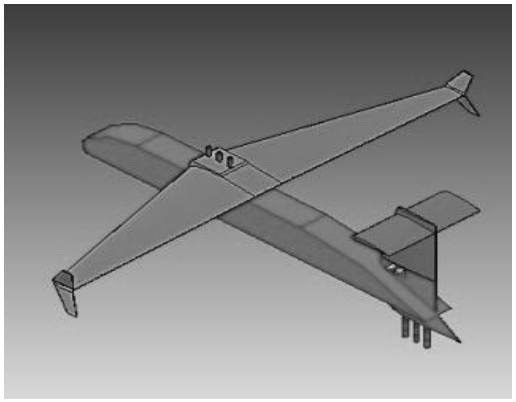

Fig. 7 Planar configuration.

References

[1] I. Kroo, Drag due to lift: Concepts for prediction and reduction, Annu. Rev. Fluid Mech. 33 (2001) 587-617.

[2] I. Kroo, Innovations in aeronautics, in: 42nd AIAA Aerospace Sciences Meeting, Reno, NV, Jan. 5-8, 2004.

[3] I. Kroo, Nonplanar wing concepts for increased aircraft efficiency, in: VKI Lecture Series on Innovative Configurations and Advanced Concepts for Future Civil Aircraft, Belgium, Jun. 6-10, 2005.

[4] L. Prandtl, Induced drag of multiplanes, NACA TN 182, 1924.

[5] E. Torenbeek, Blended-wing-body and all wing airliners, in: 8th European Workshop on Aircraft Design Education, Samara, Russia, 2007.

[6] E. Torenbeek, Synthesis of Subsonic Airplane Design: An Introduction to the Preliminary Design of Subsonic General Aviation and Transport Aircraft, with Emphasis on Layout, Aerodynamic Design, propulsion and Performance, Kluwer Academic Pub., Germany, 1982.

[7] R. Austin, Unmanned Aircraft Systems, UAVS Design, Development and Deployment, John Wiley & Sons Ltd., Chichester, Reino Unido, 2010.

[8] T.J. Mueller, J.D. DeLaurier, Aerodynamics of small vehicles, Annual Review of Fluid Mechanics 35 (2003) 89-111.

[9] J. Wolkovitch, The joined wing-an overview, Journal of Aircraft 23 (3) (1986) 161-178.

[10] L. Miranda, Boxplane Configuration for Conceptual Analysis and Initial Experimental Verification, Multidisciplinary Design Optimization Laboratory, California, 1972.

[11] L. Prandtl, Induced drag of multiplanes, NACA UK Mirror report, UK, 1924.

[12] T.V. Karman, J.M. Burgers, Aerodynamic Theory: General Aerodynamic Theory: Perfect Fluids, Springer, New York, 1935.

[13] A. Frediani, M. Gasperini, G. Saporito, A. Rimondi, Development of a Prandtl plane aircraft configuration, in: Proceedings of the 17th AIDAA Congress, Roma, Italy, 2003, pp. 2263-2276.

[14] M.M. Munk, The Minimum Induced Drag of Aerofoils, NACA report No. 121, UK, 1921.

[15] A. Frediani, The Prandtl Wing, in: VKI Lecture Series on Innovative Configurations and Advanced Concepts for Future Civil Aircraft, Belgium, Jun. 6-10, 2005.

[16] F.A. Khan, P. Krammer, D. Scholz, Preliminary aerodynamic investigation of box-wing configurations using low fidelity codes, in: Deutscher Luft-und Raumfahrtkongress, Germany, 2010.

[17] D.P. Raymer, Aircraft Design: A Conceptual Approach, American Institute of Aeronautics and Astronautics, Washington D.C., 1992.

[18] P.W. Jansen, R.E. Perez, J.R. RA Martins, Aerostructural optimization of nonplanar lifting surfaces, Journal of Aircraft 47 (5) (2010) 1490-1503.

[19] J.B. Barlow, W.H. Rae, A. Pope, Low-Speed Wind Tunnel Testing, Wiley, NY, 1999.

[20] H. Glauert, Wind Tunnel Interference on Wings, Bodies and Airscrews, Brian Pinto, London, 1933.

[21] H.H. Heyson, Rapid Estimation of Wind Tunnel Corrections with Applications to Wind Tunnel and Model Design, National Aeronautics and Space Administration, Washington D.C., 1971.

[22] T.F. Brooks, C.L. Burley, A Wind Tunnel Wall Correction Model for Helicopters in Open, Closed, and Partially Open Rectangular Test Sections, NASA TM, 1999.

[23] M. Barcala, C.C. Rejado, S. del Giudice, F.G. Agüera, A.A.R. Sevillano, Experimental investigation on box-wing configuration for UAS, in: 26th Bristol International Unmanned Air Vehicle Systems Conference, University of Bristol, UK, Apr. 11-13, 2011.

[24] F.G. Agüera, A.A.R. Sevillano, M.A.B. Montejano, J.M.H. Vicente, Systems integration in a UAS design, an example of undergraduate students' tasks, in: 2011 IEEE Global Engineering Education Conference (EDUCON). Amman, Apr. 4-6, 2011, pp. 470-476.

[25] M.A.B. Montejano, F.G. Agüera, A.A.R. Sevillano, J.C. Moreno, J.P. Álvarez, J.P.G. Pérez, et al., The application of rapid prototyping in the design of an UAV, in: 27th Congress of the International Council of the Aeronautical Sciences (ICAS-2010), Nice, France, Sept. 19-24, 2010.